Bioprocess Biosyst Eng (2011) 34:923–930
DOI 10.1007/s00449-011-0543-x

ORIGINAL PAPER

Amperometric biosensor for hydrogen peroxide based on horseradish peroxidase onto gold nanowires and TiO_2 nanoparticles

Huaan Zhong · Ruo Yuan · Yaqin Chai · Wenjuan Li · Yu Zhang · Chengyan Wang

Received: 30 December 2010 / Accepted: 4 April 2011 / Published online: 20 April 2011

Abstract An electrochemical biosensor for determination of hydrogen peroxide (H_2O_2) was fabricated, based on the electrostatic immobilization of horseradish peroxidase (HRP) with one-dimensional gold nanowires (Au NWs) and TiO_2 nanoparticles (nano-TiO_2) on a gold electrode. The nano-TiO_2 can give a biocompatible microenvironment and compact film, and the Au NWs can provide fast electron transferring rate and greatly add the amount of HRP molecules immobilized on the electrode surface. Au NWs were characterized by ultraviolet–visible spectra and transmission electron microscope. The electrode modification process was probed by cyclic voltammetry and electrochemical impedance spectroscopy. Chronoamperometry was used to study the electrochemical performance of the resulting biosensor. Under optimal conditions, the linear range for the determination of H_2O_2 was from 2.3×10^{-6} to 2.4×10^{-3} M with a detection limit of 7.0×10^{-7} M (S/N = 3). Moreover, the proposed biosensor showed superior stability and high sensitivity.

Keywords Horseradish peroxidase · TiO_2 nanoparticles · Gold nanowire · Biosensor · Hydrogen peroxide

Electronic supplementary material The online version of this article (doi:10.1007/s00449-011-0543-x) contains supplementary material, which is available to authorized users.

H. Zhong · R. Yuan (✉) · Y. Chai · W. Li · Y. Zhang · C. Wang
Chongqing Key Laboratory of Analytical Chemistry, College of Chemistry and Chemical Engineering, Southwest University, Chongqing 400715, China
e-mail: yuanruo@swu.edu.cn

Introduction

Determination of hydrogen peroxide (H_2O_2) is of great interest and importance because it is the reaction catalyzed by a large number of oxidases, and it is essential in food, industrial, environmental and pharmaceutical analyses [1]. Many analytical techniques have been developed to detect H_2O_2, for example titrimetry [2], spectrophotometry [3], chemiluminescence [4], and electrochemical methods [5, 6]. Among the various transduction methods, most are too cost and time-consuming, except for electrochemical methods. Due to their simplicity, high sensitivity and selectivity, electrochemical sensors have been extensively employed in H_2O_2 determination [7–11]. Horseradish peroxidase (HRP) has been the commonly used enzyme for the construction of a H_2O_2 biosensor. The enzyme contains heme as a prosthetic group, which is also the protein active site (with the resting state of the heme-iron: Fe^{3+}), and it can catalyze the H_2O_2 dependent one-electron oxidation of a wide variety of substrates [12]. The isoelectric point of HRP is 8.9, and it also positively changed in neutral solution [13]. Until now, considerable attention has been devoted to immobilization of HRP on electrode surface, which is one of the main factors that affect the performance of a biosensor. But the significative issue is how to improve the performances of enzyme-based H_2O_2 biosensor with novel immobilizing materials.

Thereinto, nanostructured materials have received increasing interest due to their novel optical, electrical, catalytic, magnetic properties, excellent biocompatibility, strong adsorption ability and potential applications in nanoelectronic devices [14]. Nowadays, one of nanostructured materials such as nano-TiO_2 has been proposed as a potential interface for the immobilization of biomolecules, and applied in photochemistry [15] and electrochemistry

[16]. TiO_2 colloids are facile to form porous film, and enhance the surface area. Ju et al. [17] successfully immobilized HRP in nano-TiO_2 for fabricating biosensor, which exhibited high sensitivity and a favor film-forming material. Moreover, nano-TiO_2 is a positively charged species in the pH range of 2.0–3.0 as a result of the isoelectric point of rutile titania is 5.7 [18]. So a positively charged nano-TiO_2 can adsorb negatively charged materials with electrostatic interactions. These may be very beneficial in designing electrochemical sensors.

On the other hand, the gold nanoparticle has been used in constructing electrochemical biosensors [19–21], because it has the high surface area-to-volume ratio, low resistivity and good biocompatibility and suitability. Compared with spherical nanoparticle, nanowires can load much more enzyme molecules. Nanowires are momentous class of nanoscale materials with new and important activities in the one-dimensional. Au NWs can provide a large well-defined surface area and the capacity for modification of proteins on its surface, which will adopt a more flexible orientation and result in a high amount of proteins [22]. Moreover, the electrons can be transferred fast from the electrode to the active site of the enzyme via the possible conducting channels provided with Au NWs [23, 24], which can reduce response time of biosensor. These properties make Au NWs an ideal candidate as a perfect and an eximious electrode nanostructured material.

In this paper, we attempt to combine the advantages of nano-TiO_2 and Au NWs to study the electrocatalysis of protein. Firstly, nano-TiO_2 colloids were immobilized on a gold electrode surface, because they could provide a compact film and biocompatible microenvironment. And then, Au NWs were connected with nano-TiO_2 by electrostatic interactions. Subsequently, HRP molecules were adsorbed onto the Au NWs surface via electrostatic interactions and special absorption. The electrode modification process was characterized by cyclic voltammetry and electrochemical impedance spectroscopy. The optimization of experimental conditions and the performance of the modified electrode were also investigated by chronoamperometry in details.

Experimental

Reagent and materials

Horseradish peroxidase (HRP, E.C.1.11.1.7, RZ > 3.0, 250 u/mg), titania nanoparticles (nano-TiO_2, 5%, pH 2–3), chloroauric acid ($HAuCl_4$), and sodium citrate were purchased from Sigma (St. Louis, MO, USA). Cetyltrimethylammonium bromide (CTAB) and ascorbic acid were obtained from Shanghai Chemical Reagent Co. (Shanghai, China). Hydrogen peroxide (H_2O_2 30% w/v) was obtained from Chemical Reagent Co. (Chongqing, China). Phosphate buffer solutions (PBS) with various pH values were prepared with 0.1 M KH_2PO_4 0.1 M Na_2HPO_4. The supporting electrolyte was 0.1 M KCl. Gold nanoparticles with mean size of 16 nm were produced by reducing chloroauric acid with sodium citrate at 100 °C for half an hour [25, 26]. All other reagents were of analytical grade with highest purity. All solutions were made up with twice-distilled water.

Apparatus

Cyclic voltammetry (CV), electrochemical impedance spectroscopy (EIS) and amperometric (I/t) measurements were performed using a CHI 600B electrochemical workstation (CH Instruments, Chenhua Corp., Shanghai, China) at room temperature. The three-electrode system consisted of a bare or modified gold electrode which was used as a working electrode, a saturated calomel electrode (SCE) as a reference electrode and a Pt wire counter electrode. The UV–Vis spectra was carried out in the range of 400–800 nm on a type of Lambda 17 UV–Vis 8500 (PE Co., USA) with quartz cuvette (pathlength 1 cm). The transmission electron microscope (TEM) images were obtained with a TEM (H600, Hitachi Instruments, Japan).

Synthesis of gold nanowires

Au NWs were prepared according to a literature method [27] with slight modification. In brief, the standard growth solution contained 20 mL of 0.05 M CTAB with 5 μmol $HAuCl_4$ (1.0 mL of 5 mM solution) and 5.5 μmol ascorbic acid (1.0 mL of 5.5 mM solution). To this solution was added 75 μL of 1 M NaOH while stirring, raising the pH of the solution to a value of ~5 and initiating the growth process. The growth process evolved in the solution for about 5 min, accompanied by a color change, first from the transparent to yellow orange and then to deep red.

Preparation of hydrogen peroxide biosensor

The gold electrode ($\Phi = 4$ mm) was polished successively with 0.3 and 0.05 μm Al_2O_3 before modification, rinsed with double-distilled water thoroughly, and ultrasonically cleaned in acetone and double-distilled water for 5 min, respectively.

The cleaned gold electrode was immediately coated with 5 μL of nano-TiO_2 (5%) and dried in air. After that, the electrode was immersed in the solution of Au NWs for about 8 h, and then rinsed with twice-distilled water. Finally, the Au NWs/nano-TiO_2/Au modified electrode was incubated into 2.5 mg/mL HRP solutions (PBS, pH 7) for 12 h at 4 °C to effect enzyme molecules immobilization to

the electrode surface. The schematic diagram of the stepwise procedure of the H_2O_2 biosensor was shown in Scheme 1.

Results and discussion

Characterizations of the Au NWs by UV–Vis absorption spectra and TEM

The preparation of the solution of Au NWs was a key step in this work. UV–Vis absorption spectroscopy was used to investigate the gold nanoparticles (mean size of 16 nm) and Au NWs. Figure 1 displayed the UV–Vis absorption spectra of (a) gold nanoparticles and (b) Au NWs. From (a) and (b), we could see, the optical spectrum of gold nanoparticles solution had a λ_{max} of 520 nm (Fig. 1a), which was the characteristic plasmon absorbance of unaggregated gold nanoparticles. The deep red solution of Au NWs exhibited a UV–Vis absorption peak centered at 530 nm (Fig. 1b), which was typical of colloidal gold [28]. The surface topographies of the Au NWs were investigated using TEM with images shown in Fig. 2. It can be seen that threadlike nanowires were observed with mean diameter around 17 nm. These nanowires seemed to be fabricated by coalescence of one by one spherical gold nanoparticles.

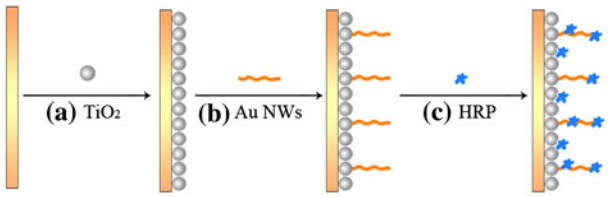

Scheme 1 Illustration of the preparation process of hydrogen peroxide biosensor

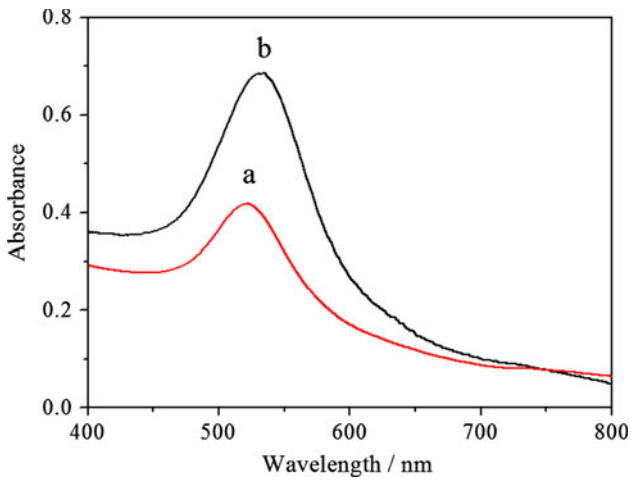

Fig. 1 UV–vis absorption spectra of **a** the gold nanoparticles, **b** Au NWs

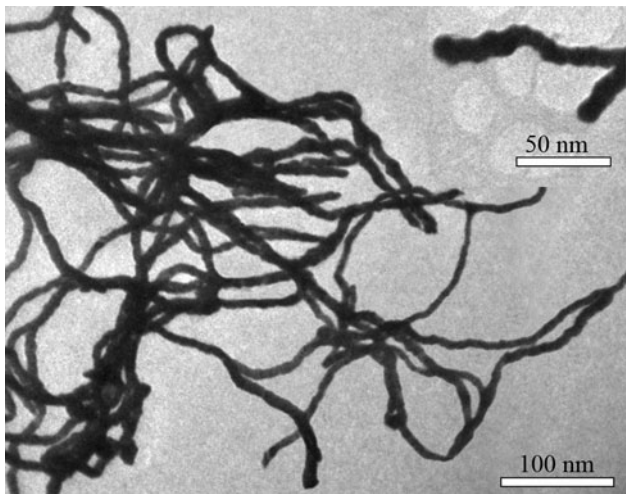

Fig. 2 TEM image of the obtained Au NWs

Electrochemical characterizations

Cyclic voltammetric characterization

The cyclic voltammetric experiments were conducted to further characterize the stepwise assembly of the H_2O_2 biosensors. Figure 3 shows the cyclic voltammograms (CVs) at differently modified electrodes in 0.1 M KCl containing 5 mM $K_3Fe(CN)_6$ at a scan rate of 50 mV/s in the range from −0.20 to 0.60 V. In Fig. 3, a pair of well-defined peaks can be observed at the bare Au electrode (Fig. 3a). In comparison with Fig. 3a, the peak currents

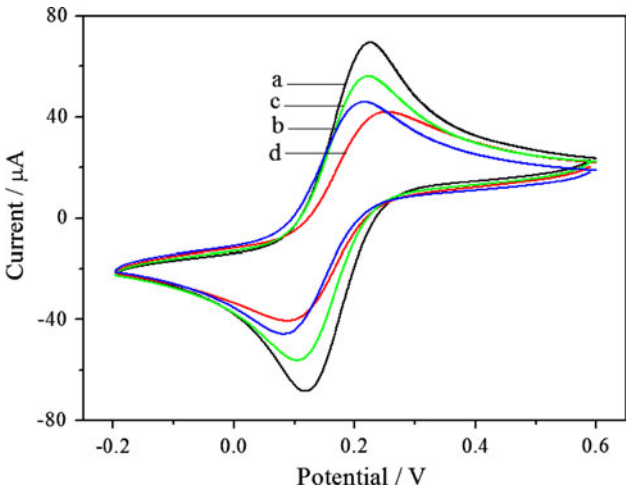

Fig. 3 Cyclic voltammograms of the flat Au electrodes (**a**), nano-TiO_2/Au (**b**), Au NWs/nano-TiO_2/Au (**c**), and HRP/Au NWs/nano-TiO_2/Au (**d**) in 0.1 M KCl containing 5 mM $K_3Fe(CN)_6$ at a scan rate of 50 mV/s

decrease after TiO_2 solution was coated on the electrode (Fig. 3b), because of the semiconductive property of nano-TiO_2. In contrast, the peak currents increase after Au NWs solution modification (Fig. 3c). The reason is that Au NWs play an important role, similarly to a conducting wire or electron-conducting tunnel, which enhances the electron-transfer kinetics. With HRP immobilization on the modified electrode surface, an obvious decrease of response current is noted (Fig. 3d), suggesting that the nonconductive property of HRP obstructs electron transfer of the electrochemical probe. On the basis of CVs' results, we might conclude that the fabricated biosensor could preliminarily be applied for detection of H_2O_2.

The electrocatalytic activity of the HRP/Au NWs/nano-TiO_2/Au towards H_2O_2 was estimated by CV. Figure 4 illustrates the CVs recorded for the proposed biosensor in 0.1 M PBS (pH 6.5) containing varied concentration of H_2O_2 in the absence of oxygen. With the increase of H_2O_2 concentration, the cathodic currents increased and the anodic currents slightly decreased, indicating a typical electrocatalytic reduction process of H_2O_2. The electrocatalytic reduction mechanism of HRP toward H_2O_2 can be explained by the following equations [29, 30]:

$$\mathrm{HRP}\left(\mathrm{Fe}^{3+}\right) + \mathrm{H_2O_2} \rightarrow \text{Compound I}\left(\mathrm{Fe}^{4+} = \mathrm{O}\right) + \mathrm{H_2O} \quad (1)$$

$$\text{Compound I}\left(\mathrm{Fe}^{4+} = \mathrm{O}\right) + \mathrm{e} + \mathrm{H}^{+} \rightarrow \text{Compound II} \quad (2)$$

$$\text{Compound II} + \mathrm{H}^{+} + \mathrm{e} \rightarrow \mathrm{HRP}\left(\mathrm{Fe}^{3+}\right) + \mathrm{H_2O} \quad (3)$$

Electrochemical impedance spectroscopy characterization

As is well known, EIS is a powerful tool for monitoring the changes of interface properties at modified electrode surfaces. The curve of the EIS includes a semicircular part and a linear part. The semicircular part at higher frequencies corresponds to the electron-transfer limited process and its diameter is equal to the electron-transfer resistance (R_{et}), which controls the electron-transfer kinetics of the redox probe at the electrode interface. Its value varies when different substances are adsorbed on the electrode surface [31]. Meanwhile, the linear part at lower frequencies corresponds to the diffusion process. In this paper, the electrochemical impedance studies of the modified electrode were carried out in 5 mM $K_3Fe(CN)_6$ and the results are shown in Fig. 5. Figure 5a shows EIS of the bare gold electrode. There is a small semicircle at high frequencies and a linear part at low frequencies, as was reported [32]. In contrast to the bare gold electrode, an increase of resistance was observed at the nano-TiO_2/Au modified electrode (Fig. 5b). The reason may be that TiO_2 as a semiconductor. Figure 5c shows that when the Au NWs/nano-TiO_2/Au modified electrode, a decreased of R_{et} can be found, implying low R_{et} to the redox probe dissolved in the electrolyte solution, because the Au NWs exhibits an excellent electrochemical activity. When the HRP molecules were adsorbed on the electrode, the interfacial resistance increased remarkably (Fig. 5d), which suggests enzyme molecules were successfully assembled on the surface of the resulting electrode. This result is consistent with the cyclic voltammetric characterization.

Electrochemical characteristics of hydrogen peroxide biosensors

The HRP/Au NWs/nano-TiO_2/Au electrode was studied further in 5 mM $K_3Fe(CN)_6$ with the change of scan rate. As shown in Fig. S1, it displays a well-defined peak shape. Increasing with scan rate form 10 to 250 mV/s, the peak

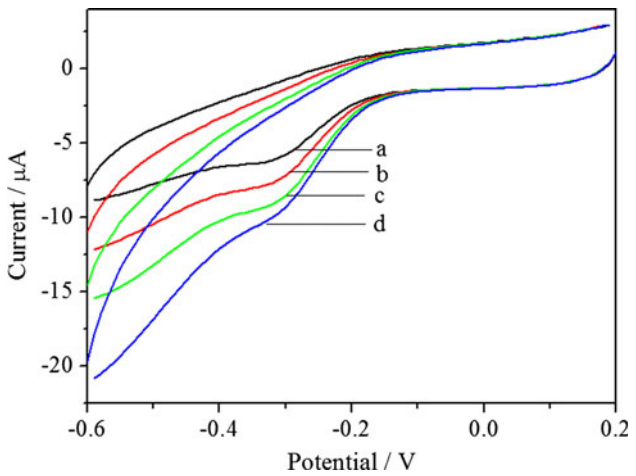

Fig. 4 CVs of the HRP/Au NWs/nano-TiO_2/Au at a scan rate of 50 mV/s in 0.1 M PBS (pH 6.5) without H_2O_2 (**a**), with 0.14 mM (**b**), 0.28 mM (**c**) and 0.56 mM (**d**), respectively

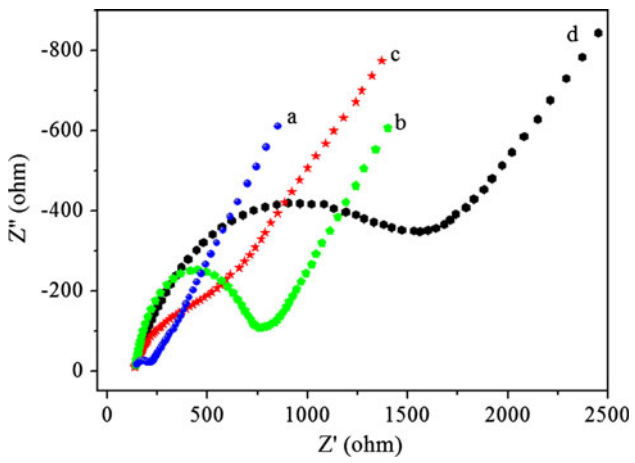

Fig. 5 EIS of the flat Au electrodes (**a**), nano-TiO_2/Au (**b**), Au NWs/nano-TiO_2/Au (**c**), and HRP/Au NWs/nano-TiO_2/Au (**d**) in 5 mM $K_3Fe(CN)_6/K_4Fe(CN)_6$ (1:1)

current increase. In addition, it is found that both cathodic and anodic peak currents increase linearly with the square root of scan rate in the range of 10 to 250 mV/s (as presented in the inset of Fig. S1), indicating it was a diffusion-controlled process.

Influence of applied potential and pH on biosensor response

Figure 6a shows the dependence of the chronoamperometric current response to constant concentration (0.07 mM H_2O_2) on the applied potential in the range from 0 to −0.40 V. From Fig. 6a, there is very little current below −0.30 V but a continuous increase from −0.30 to −0.40 V. The high operating potential results in interference from the matrix species. Therefore, −0.30 V was determined to give a good sensitivity and was selected for further study.

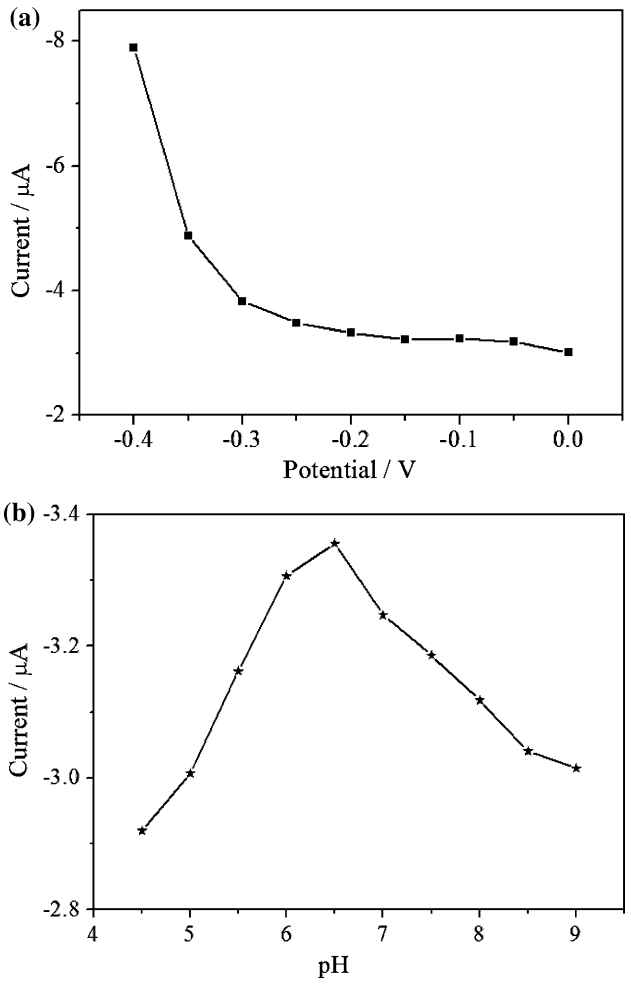

Fig. 6 Effect of potential in 0.1 M PBS (pH 6.5) (**a**), and pH of PBS (0.1 M) at applied potential of −0.30 V (**b**) on the biosensor response for 0.07 mM H_2O_2

In most cases, the pH value of the electrolyte is important for the performance of the biosensor because the activity of the enzyme is affected greatly by pH [33]. The CVs of HRP-modified electrodes also showed a strong dependence on solution pH. The change of chronoamperometric current with the pH under constant H_2O_2 concentration (0.07 mM) at the applied potential of −0.30 V is investigated in Fig. 6b. As can be seen, the response current increased from pH 4.5 and reached the maximum at pH 6.5, then decreased to pH 9.0. Strongly acidic or alkaline environments would result in the denaturation of enzyme. However, a faintly acidic solution enhances the reaction because H^+ is needed for HRP to reduce the H_2O_2 and produce water [34]. Therefore, a PBS of pH 6.5 was selected for H_2O_2 detection in this study. This finding is in agreement with the work reported for immobilized HRP on the surface of the modified gold nanoparticles stabilized [35].

Amperometric response of hydrogen peroxide biosensor

Comparative studies were carried out using different modified electrodes by successively adding H_2O_2 to a continuously stirred PBS (pH 6.5) solution at applied potential of −0.30 V. Curves a, b and c in Fig. 7 display typical current–time curves of (a) HRP/nano-TiO_2/Au, (b) HRP/nano-Au/nano-TiO_2/Au and (c) HRP/Au NWs/nano-TiO_2/Au for successive addition H_2O_2 of the same concentration (0.07 mM) at applied potential of −0.30 V. As can be shown, HRP/Au NWs/nano-TiO_2/Au (Fig. 7c) had the highest current response. Compared with it, the HRP/nano-Au/nano-TiO_2/Au (Fig. 7b) exhibited less sensitive amperometric responses to H_2O_2 when nano-Au instead of Au NWs. The reason of that Au NWs can load much more the amount of HRP molecules than nano-Au. On the other hand, the electrochemically active centre of HRP is normally buried deeply in its extended the three-dimensional structure, which makes fast electron transfer between HRP and the electrode surface prohibitively slow [36]. By Au NWs, the electrons can be transferred from the electrode to the active site of the enzyme via the possible conducting channels provided, which are within the electron-transfer distance between the electrode and HRP [37]. Without the Au NWs or nano-Au, HRP/nano-TiO_2/Au (Fig. 7a) also appeared certain electrochemical catalysis response to H_2O_2, which can be attributed to a favor film-forming and biocompatibility of nano-TiO_2. Based on these results, we confirmed that the synergistic effect of Au NWs and nano-TiO_2 made the biosensor exhibit excellent performances. The Au NWs/nano-TiO_2 can provide a congenial microenvironment for retaining the activity of the enzyme molecules to orient in conformations more favorable for electron transfer.

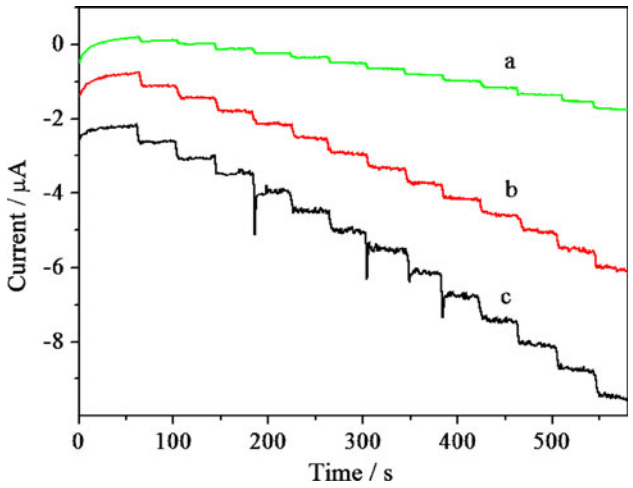

Fig. 7 Current response to successive addition of 0.07 mM H_2O_2 of (**a**) HRP/nano-TiO_2/Au, (**b**) HRP/nano-Au/nano-TiO_2/Au, and (**c**) HRP/Au NWs/nano-TiO_2/Au in 0.1 M PBS (pH 6.5) at applied potential of −0.30 V

The amperometric responses to H_2O_2 of HRP/Au NWs/nano-TiO_2/Au modified electrodes were investigated by successively adding H_2O_2 to a continuously stirred PBS solution under the optimized conditions. The typical current–time curve of the biosensor is shown in Fig. 8. Increasing the concentration of H_2O_2 added into the solution, the reduction current increase, as illustrated in Fig. 8. We used the steady-state current to plot with the concentration of H_2O_2. The response current increased linearly with the H_2O_2 concentration in the range of 2.3×10^{-6} to 2.4×10^{-3} M with a correlation coefficient of 0.997 ($n = 22$) (the inset of Fig. 8). From the slope of the calibration curve, the detection limit of 7.0×10^{-7} M is estimated at a signal-to-noise ratio of three. In addition, the biosensor shows fast response achieving 95% of the steady-state current within 5 s. The Michaelis–Menten constant (K_M^{app}), which is a reflection of both the enzymatic affinity and the ratio of microscopic kinetic constant, was calculated to be 1.27 mM according to the Lineweaver–Burk equation [38]. It was lower than the value of either previous report for the HRP/TiO_2 modified electrode (1.98 mM) [17] or for the HRP/Au colloid/cysteamine modified gold electrode (2.30 mM) [39]. This result reveals that the biosensor possesses higher enzymatic activity and the immobilized HRP shows higher biological affinity to H_2O_2. The performance of the HRP/Au NWs/nano-TiO_2 biosensor developed in this study was compared with other biosensors as listed in Table 1. This reveals that our proposed biosensor shows excellent performance in terms of low detection limit and long linear range.

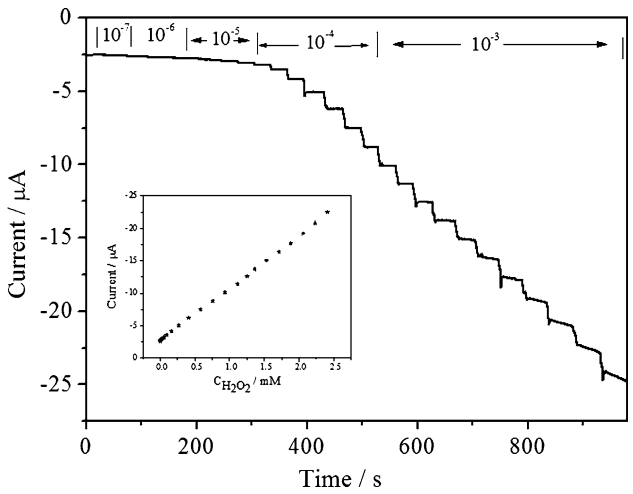

Fig. 8 Typical current–time response current of the biosensor upon successive adding different concentrations of H_2O_2 into 5 mL of pH 6.5 PBS (0.1 M) at applied potential of −0.30 V. *Inset* shows the linear calibration curve

Stability, reproducibility, and interference of the hydrogen peroxide biosensor

When stored above 0.1 M PBS (pH 6.5) at 4 °C in a refrigerator, the biosensors were stable and retained 91% of its initial activity for H_2O_2 after 1 month, indicating the H_2O_2 biosensor had a longer lifetime. The biosensor also shows good reproducibility for the determination of H_2O_2 concentration in its linear range. The relative standard deviation (RSD) is 3.5% for five successive assays at the H_2O_2 concentration of 0.25 mM.

In addition, the potential interference of some biological substance was investigated. In our experiments, the test solutions were deaerated by high pure nitrogen. Five interfering substances were used to examine whether they interfere the determination of H_2O_2 in our experiments. Experimental results were listed in Table S1. The results of the interference study showed that five interfering substances did not cause observable interference, which should be owed to the low working potential of −0.3 V used in the determination of H_2O_2.

Real sample analysis

In order to investigate the possibility of using the proposed biosensor, determination of H_2O_2 in disinfector real samples was performed by the developed H_2O_2 biosensor. For comparison, the potassium permanganate titration method as a standard method for H_2O_2 detection had been presented. Disinfector was obtained from the Hospital of Southwest University, China, which was diluted many times with 0.1 M PBS (pH 6.5). The results obtained with two methods were given in Table 2. It can be seen that the biosensor is still effective when the sample is replaced

Table 1 Comparison of performances of proposal biosensor for H_2O_2 detection with those of biosensors based on different matrices

Electrode	Linear range (mM)	Detection limit (μM)	Applied potential (V) versus SCE	R^2	References
HRP/Au NWs/TiO_2/Au	0.0023–2.4	0.7	−0.30 V	0.997	This work
HRP/Au/TiO_2 nanotube/Ti	0.005–0.4	2.0	−0.60 V versus Ag/AgCl	0.996	[40]
TiO_2 sol–gel/HRP/GCE	0.08–0.56	1.5	−0.15 V	0.9979	[17]
Nafion/HRP–GNSs–TiO_2/GCE	0.041–0.63	5.9	−0.30 V	0.999	[41]
HRP/Au NPs/SF/GCE	0.01–1.8	5.0	−0.21 V	0.9989	[42]
Au NWs sphere/GCE	0.1–0.8	1.2	−0.20 V versus Ag/AgCl	0.998	[43]
HRP–CMC–CD/Au	0.1–3.9	15.0	−0.05 V versus Ag/AgCl	0.997	[44]

Table 2 Determination the concentrations (mM) of H_2O_2 in disinfector samples

Samples number	Measured by proposed H_2O_2 biosensor		Measured by $KMnO_4$-titrated method
	(mean ± SD)[a]	R.S.D (%)	
1	0.2449 ± 0.0061	2.5	0.2563
2	0.9974 ± 0.0359	3.6	1.1835
3	1.9586 ± 0.0568	2.9	2.2157

[a] Average value from three successive measurements

from H_2O_2 solution to disinfector and accuracy of test results is reliable in a certain range. It implies that the sensing ability of this biosensor is not limited to H_2O_2 solution. It also can be used to test on medicine sample.

Conclusion

In this work, a strategy based on Au NWs/nano-TiO_2 modified gold electrode was proposed for developing an amperometric enzyme biosensor for H_2O_2. Au NWs/nano-TiO_2 provided a microenvironment around the protein to retain the enzymatic bioactivity and good electrocatalytic activity. With these advantages, comparing with the HRP/nano-Au/TiO_2 gold electrodes, the biosensor showed a broader linear range, lower detection limit, superior stability and high sensitivity. Au NWs provide a new promising platform for the development of biosensors.

Acknowledgments This work was supported by the Natural Science Foundation of Chongqing City (CSTC-2009BA1003), China and High Technology Project Foundation of Southwest University (XSGX 02), China.

References

1. Delvaux M, Walcarius A, Demoustier-Champagne S (2004) Electrocatalytic H_2O_2 amperometric detection using gold nanotube electrode ensembles. Anal Chim Acta 525:221–230
2. Hurdis E, Romeyn HJ (1954) Accuracy of determination of hydrogen peroxide by cerate oxidimetry. Anal Chem 26:320–323
3. Matsubara C, Kawamoto N, Takamura K (1992) Oxo[5, 10, 15, 20-tetra (4-pyridyl) porphyrinato] titanium (IV): an ultra-high sensitivity spectrophotometric reagent for hydrogen peroxide. Analyst 117:1781–1784
4. Hanaoka S, Lin JM, Yamada M (2001) Chemiluminescent flow sensor for H_2O_2 based on the decomposition of H_2O_2 catalyzed by cobalt(II)-ethanolamine complex immobilized on resin. Anal Chim Acta 426:57–64
5. Kim JH, Kim SH, Shiratori S (2004) Fabrication of nanoporous and hetero structure thin film via a layer-by-layer self assembly method for a gas sensor. Sens Actuators B 102:241–247
6. Santos AS, Pereira AC, Durán N et al (2006) Kubota LT. Amperometric biosensor for ethanol based on co-immobilization of alcohol dehydrogenase and Meldola's Blue on multi-wall carbon nanotube. Electrochim Acta 52:215–220
7. Gao F, Yao Z, Huang QA et al (2011) A hydrogen peroxide biosensor based on the direct electron transfer of hemoglobin encapsulated in liquid-crystalline cubic phase on electrode. Colloids Surf B: Biointerfaces 82:359–364
8. Song Y, Wang L, Ren C et al (2006) A novel hydrogen peroxide sensor based on horseradish peroxidase immobilized in DNA films on a gold electrode. Sens Actuators B 114:1001–1006
9. Ma LP, Yuan R, Chai YQ et al (2009) Amperometric hydrogen peroxide biosensor based on covalently immobilizing thionine as a mediator. Bioprocess Biosyst Eng 32:537–544
10. Gao F, Yin J, Yao Z (2010) A nanocomposite modified electrode: electrocatalytic properties and its sensing applications to hydrogen peroxide and glucose. J Electrochem Soc 157:F35–F39
11. Thiagarajan S, Su BW, Chen SM (2009) Nano TiO_2–Au–KI film sensor for the electrocatalytic oxidation of hydrogen peroxide. Sens Actuators B 136:464–471
12. Hewson WD, Hager LP (1979) In: Dolphin D (ed) "The Porphyrins". Academic Press, New York, pp 295–232
13. Jia JB, Wang BQ, Wu AG (2002) A method to construct a third-generation horseradish peroxidase biosensor: Self-assembling gold nanoparticles to three-dimensional sol–gel network. Anal Chem 74:2217–2223
14. Guo SJ, Dong SJ (2009) Biomolecule-nanoparticle hybrids for electrochemical biosensors. Trends Anal Chem 28:96–108
15. Topoglidis E, Cass AE, Gilardi G, Beaumont N, Durrant JR et al (1998) Protein adsorption on nanocrystalline TiO_2 films: an immobilization strategy for bioanalytical devices. Anal Chem 70:5111–5113
16. Li QW, Luo GA, Jun F (2001) Direct electron transfer for heme proteins assembled on nanocrystalline TiO_2 film. Electroanalysis 13:359–363
17. Yu JH, Ju HX (2002) Preparation of porous titania sol–gel matrix for immobilization of horseradish peroxidase by a vapor deposition method. Anal Chem 74:3579–3583

18. Kosmulski M, Maczka E, Rosenholm JB (2002) Isoelectric points of metal oxides at high ionic strengths. J Phys Chem B 106:2918–2921
19. Xu SY, Peng B, Han XZ (2007) A third-generation H_2O_2 biosensor based on horseradish peroxidase-labeled Au nanoparticles self-assembled to hollow porous polymeric nanopheres. Biosens Bioelectron 22:1807–1810
20. Shi AW, Qu FL, Yang MH et al (2008) Amperometric H_2O_2 biosensor based on poly-thionine nanowire/HRP/nano-Au-modified glassy carbon electrode. Sens Actuators B 129:779–783
21. Naya SI, Inoue A, Tada H (2010) Self-assembled heterosupramolecular visible light photocatalyst consisting of gold nanoparticle-loaded titanium(IV) dioxide and surfactant. J Am Chem Soc 132:6292–6293
22. Tang DP, Yuan R, Chai YQ (2008) Quartz crystal microbalance immunoassay for carcinoma antigen 125 based on gold nanowire-functionalized biomimetic interface. Analyst 133:933–938
23. Menon VP, Martin CR (1995) Fabrication and evaluation of nanoelectrode ensembles. Anal Chem 67:1920–1928
24. Wang C, Hu YJ, Lieber CM et al (2008) Ultrathin Au nanowires and their transport properties. J Am Chem Soc 130:8902–8903
25. Enustun BV, Turkevich JJ (1963) Coagulation of colloidal gold. J Am Chem Soc 85:3317–3328
26. Garbar KC, Griffith FR, Hommer MB et al (1995) Preparation and characterization of Au colloid monolayers. Anal Chem 67:735–743
27. Krichevski O, Tirosh E, Markovich G (2006) Formation of gold–silver nanowires in thin surfactant solution films. Langmuir 2:867–870
28. Sanedrin RG, Georganopoulou D, Park S et al (2005) Seed-mediated growth of bimetallic prisms. Adv Mater 17:1027–1031
29. Gu BX, Xu XC, Zhu GP et al (2009) Layer immobilized horseradish peroxidase on zinc oxide nanorods for biosensing. J Phys Chem B 113:6553–6557
30. Dimcheva N, Horozova E (2005) Horseradish peroxidase-based organic-phase enzyme electrode. Anal Bioanal Chem 382: 1374–1379
31. Liu YJ, Yin F, Long YM et al (2003) Study of the immobilization of alcohol dehydrogenase on Au-colloid modified gold electrode by piezoelectric quartz crystal sensor, cyclic voltammetry and electrochemical impedance techniques. J Colloid Interface Sci 258:75–78
32. Yuan S, Hu SS (2004) Characterization and electrochemical studies of Nafion/nano-TiO_2 film modified electrodes. Electrochim Acta 49:4287–4293
33. Paul D, Barker A, Grant M (1992) pH-Linked conformational regulation of a metalloprotein oxidation–reduction equilibrium: electrochemical analysis of the alkaline form of cytochrome c. J Am Chem Soc 114:3619–3624
34. Tangkuaram T, Ponchio C, Kangkasomboon T (2007) Design and development of a highly stable hydrogen peroxide biosensor on screen printed carbon electrode based on horseradish peroxidase bound with gold nanoparticles in the matrix of chitosan. Biosens Bioelectron 22:2071–2078
35. Zhou KF, Zhu YH, Yang XL (2010) A novel hydrogen peroxide biosensor based on Au–graphene–HRP–chitosan biocomposites. Electrochim Acta 55:3055–3060
36. Wu YH, Hu SS (2007) Biosensors based on direct electron transfer in redox proteins. Microchim Acta 159:1–17
37. Xu Q, Mao C, Liu NN (2006) Direct electrochemistry of horseradish peroxidase based on biocompatible carboxymethyl chitosan–gold nanoparticle nanocomposite. Biosens Bioelectron 22:768–773
38. Kamin RA, Willson GS (1980) Rotating ring-disk enzyme electrode for biocatalysis kinetic studies and characterization of the immobilized enzyme layer. Anal Chem 52:1198–1205
39. Xiao Y, Ju HX, Chen HY (2000) Direct electrochemistry of horseradish peroxidase immobilized on a colloid/cysteamine-modified gold electrode. Anal Biochem 278:22–28
40. Kafi AKM, Wu GS, Chen AC (2008) A novel hydrogen peroxide biosensor based on the immobilization of horseradish peroxidase onto Au-modified titanium dioxide nanotube arrays. Biosens Bioelectron 24:566–571
41. Wang Y, Ma XL, Wen Y et al (2010) Direct electrochemistry and bioelectrocatalysis of horseradish peroxidase based on gold nanoseeds dotted TiO_2 nanocomposite. Biosens Bioelectron 25: 2442–2446
42. Yin HH, Ai SY, Shi WJ et al (2009) A novel hydrogen peroxide biosensor based on horseradish peroxidase immobilized on gold nanoparticles–silk fibroin modified glassy carbon electrode and direct electrochemistry of horseradish peroxidase. Sens Actuators B 137:747–753
43. Guo SG, Wen D, Dong SJ (2009) Gold nanowire assembling architecture for H_2O_2 electrochemical sensor. Talanta 77: 1510–1517
44. Camacho C, Matias JC, Cao R et al (2008) Hydrogen peroxide biosensor with a supramolecular layer-by-layer design. Langmuir 24:7654–7657